



FPSPACK: a package of FORTRAN subroutines to manage earthquake focal mechanism data[☆]

Paolo Gasperini^{a,*}, Gianfranco Vannucci^b

^a Dipartimento di Fisica, Università di Bologna, Viale Bertini-Pichat 8, Bologna I-40127, Italy

^b Istituto Nazionale di Geofisica e Vulcanologia, Bologna, Italy

Received 12 April 2002; received in revised form 11 April 2003; accepted 16 April 2003

Abstract

Earthquake fault plane solutions (FPSs) are routinely computed on the basis of various techniques and are reported in the literature with a wide range of formats and conventions. Although the equations relating the various parameters are well known and relatively simple, their practical application often arise to numerical singularities and indeterminations that sometimes are not well known by the authors and thus may result in wrong or inaccurate reporting of parameters. Such inaccuracies and mistakes affect about 40% of the published data we have examined to test our programs. Moreover the current use, in the seismological community, of at least two different coordinate systems to represent the Cartesian components of vectorial and tensorial quantities is a further cause of confusion. In order to simplify the management of such data, we have prepared a structured package of FORTRAN 77 subroutines performing almost all of the possible computations and conversions among different parameters and coordinate systems. The package has been extensively tested with the data of a revised database of FPS of Italy and surrounding regions (presented in a companion paper) as well as of CMT solutions included in the Harvard catalog.

© 2003 Elsevier Ltd. All rights reserved.

Keywords: Fault plane solutions; FORTRAN 77; Centroid moment tensor; Deformation axes; Nodal planes

1. Introduction

The relations among parameters of earthquake focal mechanisms are matter for seismology textbooks and should be well known to every investigator that approaches the study of seismologically related problems. However, the scarce habit of many geo-scientists in dealing with angular and tensorial quantities resulted in the fact that, past years, the published focal mechanisms parameters sometimes contain inaccuracies and inconsistencies, even in articles appearing on authoritative journals.

In the framework of a companion study devoted to the construction of a catalog of fault plane solution (FPS) for Italy and surrounding regions (Vannucci and Gasperini, 2003), we have found that about 40% of the processed data contain wrong, inconsistent or insufficient parameters. The most frequent errors encountered are rotations of 90° or 180° of the fault strike and/or rake, but also inconsistencies between fault planes and *P*- and *T*-axis, as well as deviations from orthogonality between planes and among axes were also commonly found.

With this work we want to make available the routines we have written to check and recompute the parameters of events included in the above database, in order to simplify the approach to these problems even for investigators who have less expertise on seismological and computational problems.

In order to simplify and make more reliable the testing of the code we have rigorously structured the

[☆] Code on server at <http://www.iamg.org/CGEditor/index.htm>.

*Corresponding author.

E-mail addresses: paolo@ibogfs.df.unibo.it (P. Gasperini), gfranco@ibogfs.df.unibo.it (G. Vannucci).

package, subdividing the computations into simple elementary tasks performed by different subroutines. The formulas we have used are derived from common seismological textbooks like Aki and Richards (1980) or Lay and Wallace (1995) and are described in Appendix A. Almost all computations are done in the standard Cartesian coordinate system defined by Aki and Richards (1980) (now on AR system), where the x -axis is directed northward, the y -axis eastward and the z -axis downward (black arrows in Fig. 1). We also provide some routines to convert the seismic moment tensor components to and from the coordinate system used by the Harvard CMT catalog (Dziewonski et al., 1981 and subsequent quarterly papers on Physics of the Earth and Planetary Interior journal, now on Harvard system), where x -axis is southward, y -axis eastward and z -axis upward (radial) (gray arrows in Fig. 1).

The package is written in standard FORTRAN 77 and thus can be compiled and used without any adaptation, both on workstations and personal computers, by common FORTRAN 77 compilers (i.e. GNU g77 or Compaq Visual Fortran). All floating-point variables are in single precision (REAL*4) as we have verified that the use of double precision does not modify the results of computations within the required accuracy. For almost all of the subroutines included in the package the last argument returns an error code. If the code is different from 0 the values of other output arguments are not significant. Most error codes concern the range of input parameters but also the orthogonality

of axes and planes and the symmetry of the moment tensor are checked.

2. Structure of the package

The package is structured in three groups of subroutines: basics, composites and utilities. The first group includes procedures that perform elementary computations and conversions. In particular, we included in this group the routines which convert planes and axes from angular to Cartesian representation and vice versa, compute principal axes of moment tensor, compute moment tensor component of a double-couple from outward normal and slip vector, and convert from the AR to the Harvard coordinate system. Note that if not otherwise specified, the AR coordinate system is used.

- (1) PL2ND—Compute Cartesian components of outward normal and slip vectors from strike, dip and rake of a nodal plane.
- (2) ND2PL—Compute strike, dip and rake of a nodal plane from Cartesian components of outward normal and slip vectors.
- (3) AX2CA—Compute Cartesian components of an axis (P , T or B) from plunge and trend.
- (4) CA2AX—Compute plunge and trend of an axis from Cartesian components.
- (5) PT2ND—Compute Cartesian components of outward normal and slip vectors from P - and T -axis Cartesian components.
- (6) ND2PT—Compute Cartesian components of P -, T - and B -axis from Cartesian components of outward normal and slip vectors.
- (7) AR2PT—Computes Cartesian components of P -, T - and B -axis from moment tensor Cartesian components.
- (8) ND2AR—Computes moment tensor Cartesian component for a double couple from outward normal and slip vectors.
- (9) AR2HA—Converts moment tensor Cartesian components from the Aki-Richards to the Harvard CMT coordinate systems and vice versa.

The second group of routines includes derived procedures that are a composition of basic functions. Among them we can mention the routines to compute angular parameters of axes and planes from the moment tensors, to compute the parameters of a plane from the other one, to compute axes from planes and vice versa.

- (1) ND2HA—Computes seismic moment tensor Cartesian component for a double couple in the Harvard CMT coordinate system from the outward normal and slip vectors. Calls ND2AR and AR2HA.

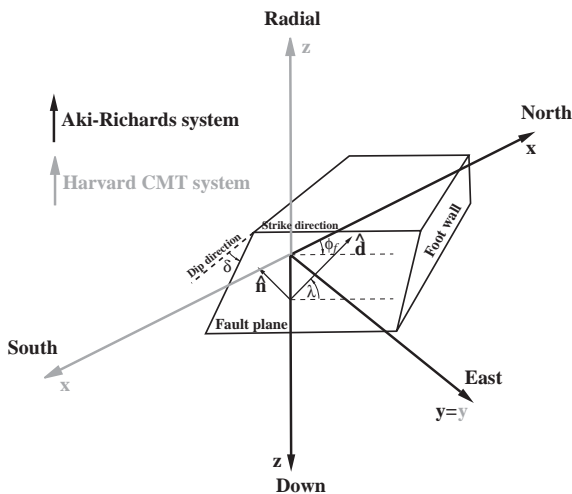


Fig. 1. Fault plane geometry and coordinate systems. Black arrows correspond to axes of standard system defined by Aki and Richards (1980), whereas gray ones to system used by Harvard CMT project. \hat{n} and \hat{d} indicate outward normal and displacement vectors, respectively. ϕ_f is nodal plane strike, δ is dip and λ is rake.

- (2) PL2PL—Computes the parameters of one nodal plane from the other one. Calls PL2ND then ND2PL, swapping the outward normal with the slip vectors.
- (3) PL2PT—Computes P -, T - and B -axis from one nodal plane (with rake). Calls PL2ND then ND2PT and CA2AX for the three axes.
- (4) PT2PL—Computes nodal planes from P - and T -axis. Calls AX2CA for the two axes then PT2ND and ND2PL
- (5) AR2PLP—Computes strike, dip and rake of the two nodal planes of the best double couple and trend and plunge of P -, T - and B -axis, from the moment tensor Cartesian components. Calls AR2PT, PT2ND, ND2PL (for both planes) and CA2AX (for the three axes).
- (6) HA2PLP—Computes strike, dip and rake of the two nodal planes of the best double couple and the trend and plunge of the P -, T - and B -axis, from the moment tensor Cartesian components in the Harvard CMT coordinate system. Calls AR2HA and AR2PLP.
- (7) PL2AR—Computes moment tensor Cartesian components of a double couple from strike, dip and rake of a nodal plane. Calls PL2ND and ND2AR.
- (8) PL2HA—Computes moment tensor Cartesian components in the Harvard CMT coordinate system of a double couple from strike, dip and rake of a nodal plane. Calls PL2AR and AR2HA.
- (9) PT2AR—Computes moment tensor Cartesian components for a double couple, from P - and T -axis. Calls AX2CA (for both axes) then PT2ND and ND2AR.
- (10) PT2HA—Computes moment tensor Cartesian components in the Harvard CMT coordinate system for a double couple, from the P - and T -axis. Calls PT2AR and AR2HA;
- (3) ANGLEA—Computes the angle (in degrees) between two axes (given with plunge and trend).
- (4) ANGLES—Compute the angles (in degrees) between nodal planes and slip directions.
- (5) NORM—Computes Euclidean norm and normalized components of a vector.
- (6) VECPRO—Computes vector product of two vectors (given in Cartesian components).
- (7) INVERT—Reverses the direction of a vector.
- (8) HATENS—Builds the moment tensor in the Harvard CMT coordinate system from his six independent components Mrr, Mss, Mee, Mrs, Mre and Mse
- (9) TENSHA—Returns six independent components from the moment tensor in the Harvard CMT coordinate system.
- (10) FPSSET—Defines constants (i.e. input ranges and tolerances) used throughout the package.

3. Testing of the code

This package was extensively tested using the focal mechanisms included in the above cited FPS database as well as with the CMT solutions of the Harvard CMT catalog (that can be downloaded from the web¹). We also tested the internal consistency of different computations performed by the package over the whole range of fault plane parameters ($0^\circ \leq \text{strike} \leq 360^\circ$, $0^\circ \leq \text{dip} \leq 90^\circ$, and $-180^\circ \leq \text{rake} \leq 180^\circ$). We computed axis orientations and tensor components, by varying the orientation of a nodal plane and of the corresponding slip direction and then recomputing back the parameters of the plane. The differences between starting and recomputed parameters were found to be in all the cases lower than 1° .

For the data of the FPS database we compared the parameters of planes computed from axes with the original one reported on papers and vice versa. For the CMT catalog we compared the principal axes and the nodal planes of the best double-couple computed from the moment tensor components with the ones reported by the catalog. We found that our computations coincide within a reasonable tolerance (usually 3° both for planes and axes) with the data reported by the majority of the papers contributing to the FPS database as well as the data of more than 99% of the Harvard CMT catalog solutions (in all more than 18 000). For the latter data set, the differences between original and recomputed strike dip and rake (see Table 1) exceed 3° only for 38 earthquakes (0.2%) while for the parameters of the axes, the solutions showing differences larger than

The third group includes utility routines performing simple vectorial or tensorial operations like the computation of eigenvalues and eigenvectors of a 3×3 tensor, the vector product, the angle between two vectors, etc. As well in this group we included two very simple routines to import and export the Harvard CMT components.

- (1) AVEC—Returns eigenvalues and eigenvectors of a 3×3 matrix in decreasing order of modulus magnitude. It calls the IMSL Library routine EVCSF (included in the Visual Fortran kit). If this library is not available to the user, the call to EVCSF can be easily replaced with another similar routine (e.g. Press et al., 1989).
- (2) ANGLE—Computes the angle (in degrees) between two vectors.

¹Harvard Centroid Moment Tensor project. <http://www.seismology.harvard.edu/projects/CMT/>.

Table 1

Results of comparison between reported and recomputed parameters for Harvard CMT catalog

Parameters	Difference $\leq 3^\circ$	$3^\circ < \text{difference} \leq 6^\circ$	Difference $> 6^\circ$
Strike, dip, rake of planes	18058 (99.79%)	24 (0.13%)	14 (0.08%)
Plunge and trend of axes	17966 (99.28%)	82 (0.45%)	48 (0.27%)

3° are 130 (0.7%). For most of these deviant solutions the dip and plunge angles closely approach the critical values of 0° and 90° , hence the limited accuracy of the input data prevents a reliable comparison in terms of angular parameters.

A more significant discrepancy affects the orientations of two deformation axes and consequently of the best double-couple nodal planes for about a dozen of solutions (listed in Fig. 2). All of these focal mechanisms are quite peculiar as two eigenvalues of the moment tensor have rather close values. For those who are not aware of the Harvard CMT catalog format, it may be useful to recall that each solution is reported on four lines and that the six independent tensor components and corresponding errors are reported in the third line (fields 5–16), while the eigenvalues and the corresponding eigenvectors (given as plunge and trend) of the moment tensor (fields 1–9) as well as the nodal plane parameters (fields 11–16) are reported in the fourth line.

This relatively unusual form of moment tensor reflects a strong deviation from the double couple and could indicate a pure tensional or compressive mechanism. Alternatively this might be the result of bad conditioning of the CMT solution due to the heterogeneity of the velocity structure (i.e. laterally varying) or to the complexity of the source (i.e. non-planar fault). These kind of mechanisms can be represented by Compensated Linear Vector Dipoles (CLVDs) which have one dipole of strength 2 in the direction of one eigenvector and two dipoles of unit strength in the direction of the other eigenvectors (Lay and Wallace, 1995, p. 345). In the case of a pure CLVD mechanism the nodal planes are not univocally defined and thus a best double couple could not be computed.

As an example we show with detail the comparison between our computations and the angular parameters reported on the catalog for the fourth mechanism in Fig. 2. In the AR system the moment tensor is

$$M_{ij} = \begin{pmatrix} -2.70 & 1.12 & 1.89 \\ 1.12 & 1.53 & -0.35 \\ 1.89 & -0.35 & 1.16 \end{pmatrix} \times 10^{23}. \quad (1)$$

The eigenvalues and eigenvectors resulting from our computations are reported in Table 2 compared with the original parameters given by the CMT catalog. As well the same comparison is done for nodal plane parameters in Table 3. We can note how the three eigenvalues and

the P -axis orientation are quite similar, while we can see a rotation of about 27° for the orientation of the T - and B -axis and the same rotation also affects the two nodal planes as well. We have verified that in both cases the deviations from orthogonality of axes and planes are smaller than 1° .

We believe it to be unlikely that the cause of this discrepancy, limited to so few and peculiar cases, is due to a bug in our code or in the Harvard one. We can hypothesize instead that the computation of the eigenvalues and particularly of the eigenvectors of the moment tensor becomes inaccurate when the input matrix approaches the critical form, similar to a CLVD, with two coincident eigenvalues. In the case of exact coincidence we would have in fact a single infinity of eigenvectors (all the possible directions perpendicular to the eigenvector of the third eigenvalue are eigenvectors of the moment tensor). In this critical situation, the accuracy of only two decimal digits given by the CMT catalog for the tensor components is not sufficient to allow a reliable estimate of the other two orientations. We must also note that all of the events of Fig. 1 have magnitude $M_w \cong 5$ (that is at the lower threshold of the CMT catalog) and relatively high uncertainties of the moment tensor components. This could even suggest that their deviations from the double couple could be somehow due to a low conditioning of the CMT solution.

To test the effects of the rounding of angular parameters and moment tensor components, we repeated our consistency tests by artificially rounding the computed plane and axes parameters to the nearest integer and the tensor components to the nearest second decimal digits. We found that deviations between original and recomputed parameters larger than 3° occur systematically for dip angles lower than 5° and sporadically up to 15° . These differences in the parameters do not reflect strong deviations for the true orientation of planes but, however, make a direct comparison of real solutions difficult.

4. Concluding remarks

Although the library of subroutines presented in this work does not perform particularly original or complex computations, we believe that it can be very useful to every geological and geophysical investigator to save

B041682A	04/16/82	08:14:29.8	-7.41	128.59	148.05	40.0	BANDA SEA
PDE BW:	8 12 45	MW: 0 0 0	DT=	-3.4 1.3 -7.48	0.10 128.51 0.17	144.6 6.8	
DUR	1.0 EX 23	3.01 0.49 -1.55	0.70 -1.47	0.86 -1.16	0.61 1.05	0.71 3.50	0.74
	3.31 79 225	1.99 0 135	-5.30 11 45	4.30 135	34 90	315 56	90
B031687D	03/16/87	14:35:45.5	-14.60	167.24	188.05	0.0	VANUATU ISLANDS
PDE BW:	8 13 45	MW: 0 0 0	DT=	-5.3 2.6 -14.79	0.23 167.44 0.21	162.6 4.7	
DUR	1.4 EX 23	5.55 0.67 -2.64	1.27 -2.91	1.30 -0.99	0.91 -0.47	0.81 0.11	1.22
	5.69 83 155	-2.75 7 0	-2.94 3 270	4.31 352	42 80	186 49	99
B040893D	04/08/93	19:13:14.4	18.37	-71.15	33.05	14.7	DOMINICAN REPUBLIC REG.
PDE BW:	15 18 45	MW: 0 0 0	DT=	1.4 1.1 18.40	0.11 -71.46 0.12	15.0 0.0	
DUR	1.0 EX 23	-0.47 0.25 -3.17	0.31 3.64	0.29 -5.84	1.11 1.22	1.50 1.62	0.33
	4.17 52 180	3.99 6 278	-8.16 38 12	6.16 139	9 131	277 83	84
B043093F	04/30/93	14:16:35.0	-6.04	130.30	110.05	10.0	BANDA SEA
PDE BW:	10 12 45	MW: 0 0 0	DT=	0.0 1.1 -6.04	0.00 130.30 0.00	118.7 7.1	
DUR	1.0 EX 23	1.16 0.67 -2.70	0.66 1.53	1.23 1.89	0.42 0.35	1.04 -1.12	0.75
	1.94 68 0	1.79 5 258	-3.73 22 167	2.83 248	24 78	80 67	95
B051393F	05/13/93	23:41:38.3	55.02	-160.18	33.05	34.6	ALASKA PENINSULA
PDE BW:	9 10 45	MW: 0 0 0	DT=	4.8 1.7 54.89	0.17 -159.84 0.21	40.8 10.3	
DUR	1.0 EX 23	2.58 0.39 -2.22	0.42 -0.37	0.50 1.94	0.95 1.63	1.96 -3.76	0.78
	3.34 73 322	2.58 0 232	-5.92 17 142	4.63 232	28 90	52 62	90
B032494C	03/24/94	18:40:53.4	8.12	126.61	33.05	14.2	MINDANAO, PHILIPPINE ISL
PDE BW:	10 15 45	MW: 0 0 0	DT=	6.4 0.8 8.31	0.09 126.36 0.15	33.3 11.3	
DUR	1.4 EX 23	-3.93 1.15 2.36	0.63 1.58	1.58 -1.92	1.82 2.30	1.37 0.80	0.83
	2.92 14 175	2.41 20 270	-5.33 65 52	4.12 239	35 -126	101 62	-67
B121197F	12/11/97	18:47:09.8	-6.20	101.01	33.05	0.4	SOUTHWEST OF SUMATERA
PDE BW:	15 21 45	MW: 0 0 0	DT=	1.1 0.7 -6.28	0.13 100.66 0.09	21.3 7.7	
DUR	1.0 EX 23	-2.87 0.42 1.22	0.38 1.64	0.46 0.42	1.30 -0.49	1.21 -4.22	0.62
	5.70 4 46	-2.79 0 136	-2.91 86 226	4.31 136	41 -90	316 49	-90
B040498B	4/ 4/98	14:42:52.5	-3.72	-77.39	114.24	90.0	PERU-ECUADOR BORDER REGI
PDE BW:	13 13 45	MW: 0 0 0	DT=	4.7 0.8 -3.76	0.16 -77.10 0.09	117.4 6.7	
DUR	1.0 EX 23	-3.32 0.59 -1.52	1.16 4.84	0.93 -1.00	1.97 2.04	1.59 -3.79	0.90
	7.10 12 245	-3.28 0 155	-3.82 78 65	5.46 335	33 -90	155 57	-90
B053099C	5/30/99	13:23:56.8	-2.14	125.12	33.05	0.0	CERAM SEA
PDE BW:	15 17 45	MW: 0 0 0	DT=	1.5 1.5 -1.97	0.13 125.25 0.11	63.2 9.6	
DUR	1.0 EX 23	2.38 0.49 -2.86	0.49 0.47	0.86 2.43	1.36 -1.76	0.78 4.84	0.78
	3.93 0 126	3.32 73 36	-7.25 17 216	5.59 259	78 -12	352 78	-168
B091599B	9/15/99	19:38:56.2	44.36	149.43	33.05	0.4	KURIL ISLANDS
PDE BW:	9 12 45	MW: 0 0 0	DT=	3.4 1.4 44.69	0.22 149.69 0.34	33.0 0.0	
DUR	1.0 EX 23	2.76 0.58 -1.85	0.59 -0.91	0.82 0.50	2.22 2.39	1.19 0.21	0.72
	3.99 63 282	-1.90 5 182	-2.09 26 90	3.04 169	19 76	4 71	95
B092199G	9/21/99	18:18:40.0	24.06	121.15	33.04	90.0	TAIWAN
PDE BW:	7 7 45	MW: 0 0 0	DT=	2.3 2.3 24.12	0.21 120.71 0.46	33.0 0.0	
DUR	1.0 EX 23	-2.85 1.57 -4.20	1.04 7.05	2.50 0.97	1.87 -3.62	2.61 -3.27	0.82
	9.11 18 75	-4.03 72 270	-5.08 4 166	7.10 212	74 9	119 81	164
B021700C	02/17/00	22:00:30.3	-5.03	153.10	65.45	14.8	NEW IRELAND REGION
PDE BW:	27 43 45	MW: 0 0 0	DT=	0.2 0.5 -4.73	0.08 153.56 0.04	65.0 0.0	
DUR	1.0 EX 23	4.57 0.45 5.21	0.94 -9.77	0.69 0.13	0.70 1.52	0.71 -1.77	0.49
	5.41 0 187	4.73 84 277	-10.14 6 97	7.78 232	86 -176	142 86	-4
B031101B	03/11/01	07:06:03.5	-4.26	89.08	10.04	94.9	SOUTH INDIAN OCEAN
PDE BW:	18 24 45	MW: 0 0 0	DT=	2.9 0.9 -3.96	0.12 88.80 0.15	15.0 0.0	
DUR	1.0 EX 23	1.92 0.47 -0.17	0.51 -1.75	0.78 2.80	1.32 3.33	1.73 -5.05	0.38
	4.15 0 221	3.83 66 311	-7.98 24 131	6.06 268	73 -163	173 73	-17

Fig. 2. Centroid moment tensor solutions from Harvard CMT catalog,¹ strongly deviating from double couple, for which discrepancies are found in derived nodal planes and deformation axes parameters. Each solution is represented by four lines: six independent moment tensor component and corresponding errors are reported in third line (fields 5–16), whereas in fourth line there are eigenvalues and eigenvectors (fields 1–9) and best double-couple nodal planes (fields 11–16).

programming time and to minimize computational errors and inaccuracies. In particular, the very intensive testing we have done should grant that its use be free from indeterminations, and numerical errors that might occur for certain parameter values.

The comparison with the computations performed by the Harvard CMT team has shown that some amount of

discrepancies (for less than 1% of the solutions) is not eliminable when the input data are reported with poor accuracy (usually 1°). In fact, while the two-way computations made on simulated input data, with the full accuracy of single precision floating-point variables, perfectly reproduce the starting input values, this does not occur for rounded synthetic data as well as for real

Table 2

Comparison between recomputed and original eigenvalues and eigenvector of moment tensor for fourth CMT solution in Fig. 2

Axis	Recomputed			CMT catalog		
	Eigenvalue	Plunge	Trend	Eigenvalue	Plunge	Trend
Most tensional (<i>T</i>)	1.98×1023	52	46	1.94×1023	68	0
Null (<i>B</i>)	1.74×1023	30	269	1.79×1023	5	258
Most compressive (<i>P</i>)	-3.73×1023	21	167	-3.73×1023	22	167

Table 3

Comparison between recomputed and original nodal plane parameters for fourth CMT solution in Fig. 2

Plane	Recomputed			CMT catalog		
	Strike	Dip	Rake	Strike	Dip	Rake
<i>A</i>	216	35	31	248	24	78
<i>B</i>	100	73	121	80	67	95

data taken from the CMT catalog. In fact, when the dip or plunge angles are close to critical values of 0° or 90° , the small deviations from the orthogonality of planes and axes, due to the rounding to the nearest integer of the input values, or even the limited resolution of moment tensor components, may induce significant differences for the derived parameters with respect to the original computation done in full accuracy. The situation is similar, although more critical, for the moment tensor solutions approaching a CLVD-type source with two eigenvalues close to each other. Here the accuracy of two decimal digits for the tensor components might be the cause of observed deviations in the orientation of planes and axes up to some tens of degrees.

In almost all the subroutines of the package the mutual consistency of input parameters and their belonging to the definition ranges is checked, but to avoid wrong rejections due to bad rounding of floating-point variables we use some tolerance thresholds. In particular, we allow deviations from orthogonality of planes and/or axes up to 2° as well as we allow a small ($<0.001^\circ$) overtaking of the upper (90°) and lower (0°) thresholds for the dip and plunge angles and small ($<0.0001^\circ$) deviation from the symmetry of the moment tensor components. These thresholds can be easily modified by the user in subroutine FPSSET.

The use of the package is very simple so we have not prepared a detailed write up or a manual for the users. However, the calling sequence, the arguments and the error codes can be found on comment lines located at the beginning of the source of each subroutine.

Acknowledgements

This work was performed in the ambit of the Framework Project 2000/2002 of the Italian Gruppo Nazionale Difesa dai Terremoti (GNDT) devoted to the revision of seismic hazard assessment in Italy. It was also supported by the Istituto Nazionale di Geofisica and Vulcanologia (INGV) and by the Italian Ministry of the Education, University and Research (MIUR), research grants: Cofin 1999 and 2001. We thank Dario Albarello and Silvia Pondrelli for useful discussions and suggestions.

Appendix A. Formulas used to compute parameters of fault planes, deformation principal axes and moment tensor

A FPS representative of a double-couple mechanism can be completely defined by the three angular parameters of one of the two nodal planes (see Fig. 1):

- (1) The dip (or plunge) angle δ , that is the angle formed by the Earth surface and the nodal plane. It can be computed as the angle between two vectors, lying on the Earth surface and on the nodal plane, respectively, both directed along the maximum slope of the fault (dip direction). It may vary from 0° to 90° .
- (2) The strike (or azimuth) angle ϕ_f . It represents the azimuth of the fault trace and corresponds to the clockwise angle, computed on the Earth surface, between the direction of the North and the direction of maximum dip minus 90° . It may vary over the range 0 – 360° (or equivalently -180° to 180°).

(3) The rake (or slip) angle λ . That is the counter-clockwise angle, computed on the nodal plane, between the strike vector and the slip vector representing the direction of motion of the block located above the plane (hanging wall) with respect to the block located below it (foot wall). It may vary over the range -180° to 180° (or $0-360^\circ$).

Some ambiguities arise when the plane is exactly vertical ($\delta=90^\circ$) or exactly horizontal ($\delta=0^\circ$). In the first case, two values of the strike differing by 180° and two corresponding values of the rake (also differing by 180°) are representative of the mechanism. In the second case, the strike is undefined and can assume any value between 0° and 360° and the rake varies correspondingly.

The FPS can be completely defined also indicating the orientation of both of the axes of maximum compression (P) and tension (T). These are usually given specifying two angles:

- (1) The plunge angle γ : That is the inclination of the axis with respect to the horizontal direction. It ranges from 0° to 90° .
- (2) The trend angle α : That is the clockwise angle, computed on the Earth surface, between the direction of North and the surface projection of the axis versor. It may vary over the range from 0° to 360° .

Even in this case we have an ambiguity in the definition when the axis is exactly vertical ($\gamma=90^\circ$) or exactly horizontal ($\gamma=0^\circ$). In the former case the trend is undefined while in the latter one, two values of the trend, differing by 180° , are both representative of the orientation of the axis.

If the strike dip and rake of a nodal plane are known, we can compute the Cartesian components of the outward normal \hat{n} and of the displacement (slip) \hat{d} versors in the coordinate system (see Fig. 1) defined by Aki and Richards (1980) (AR system) using the following formulas:

$$\begin{aligned} n_x &= -\sin \delta \sin \phi_f, \\ n_y &= \sin \delta \cos \phi_f, \\ n_z &= -\cos \delta, \end{aligned} \tag{A.1}$$

$$\begin{aligned} d_x &= \cos \lambda \cos \phi_f + \cos \delta \sin \lambda \sin \phi_f, \\ d_y &= \cos \lambda \sin \phi_f - \cos \delta \sin \lambda \cos \phi_f, \\ d_z &= -\sin \delta \sin \lambda \end{aligned} \tag{A.2}$$

from which we can derive the outward normal \hat{n}' and the slip vector \hat{d}' of the second plane as $\hat{n}' = \hat{d}$ and $\hat{d}' = \hat{n}$. Hence we can compute the angular representation of the second plane, taking care that the normal vector is

upward ($n'_z < 0$, otherwise both \hat{n}' and \hat{d}' must be reversed), as

$$\left. \begin{aligned} \delta &= \arccos(-n'_z), \\ \phi_f &= \arctan\left(\frac{-n'_x}{n'_y}\right), \\ \lambda &= \arctan\left(\frac{-d'_z/\sin \delta}{d'_x \cos \phi_f + d'_y \sin \phi_f}\right), \end{aligned} \right\} \hat{n}'_z \neq -1, \\ \left. \begin{aligned} \delta &= 0, \\ \phi_f &= 0, \\ \lambda &= \arctan\left(\frac{-d'_y}{d'_x}\right), \end{aligned} \right\} \hat{n}'_z = -1. \tag{A.3}$$

Note that the relative signs of numerator and denominator of the argument of arctangent function allow computing the strike and the rake over the ranges $0^\circ-360^\circ$ and -180° to 180° .

The Cartesian components of maximum compression \hat{p} , maximum tension \hat{i} and null \hat{b} axis versors can be computed from the upward normal \hat{n} and of the displacement (slip) \hat{d} versors as

$$p_i = \frac{n_i - d_i}{\sqrt{(n_k - d_k)(n_k + d_k)}} = \frac{n_i - d_i}{\sqrt{2}}, \tag{A.4}$$

$$t_i = \frac{n_i + d_i}{\sqrt{(n_k + d_k)(n_k - d_k)}} = \frac{n_i + d_i}{\sqrt{2}}, \tag{A.5}$$

$$b_i = e_{ijk} n_j d_k, \tag{A.6}$$

where e_{ijk} is the permutation tensor.

From the above expressions we can get the angular representation of axes, now taking care that the versor directions are downward ($p_z > 0, t_z > 0, b_z > 0$, otherwise they must be reversed)

$$\begin{aligned} \gamma_P &= \arcsin(p_z), & \alpha_P &= \arctan\left(\frac{p_y}{p_x}\right), \\ \gamma_T &= \arcsin(t_z), & \alpha_T &= \arctan\left(\frac{t_y}{t_x}\right), \\ \gamma_B &= \arcsin(b_z), & \alpha_B &= \arctan\left(\frac{b_y}{b_x}\right). \end{aligned} \tag{A.7}$$

On the other hand, if the angular representation of the P - and T - axis are known we can compute their Cartesian component as

$$\begin{aligned} t_x &= \cos \gamma_T \cos \alpha_T, \\ t_y &= \cos \gamma_T \sin \alpha_T \\ t_z &= \sin \gamma_T, \end{aligned} \tag{A.8}$$

$$\begin{aligned} p_x &= \cos \gamma_P \cos \alpha_P, \\ p_y &= \cos \gamma_P \sin \alpha_P, \\ p_z &= \sin \gamma_P, \end{aligned} \tag{A.9}$$

then the Cartesian component of outward normal and slip versors are given by

$$\begin{aligned} n_i &= \frac{-(t_i + p_i)}{\sqrt{(t_k + p_k)(t_k + p_k)}} = \frac{-(t_i + p_i)}{\sqrt{2}}, \\ d_i &= \frac{-(t_i - p_i)}{\sqrt{(t_k - p_k)(t_k - p_k)}} = \frac{(t_i - p_i)}{\sqrt{2}}. \end{aligned} \tag{A.10}$$

Note that in this case the normal is certainly upward. From the above versors we can compute the angular representation of the first plane as

$$\left. \begin{aligned} \delta &= \arccos(-n_z), \\ \phi_f &= \arctan\left(\frac{-n_x}{n_y}\right), \\ \lambda &= \arctan\left(\frac{-d_z/\sin\delta}{d_x \cos\phi_f + d_y \sin\phi_f}\right), \end{aligned} \right\} \hat{n}_z \neq -1, \\ \left. \begin{aligned} \delta &= 0, \\ \phi_f &= 0, \\ \lambda &= \arctan\left(\frac{-d_y}{d_x}\right), \end{aligned} \right\} \hat{n}_z = -1. \tag{A.11}$$

and of the second plane using Eq. (A.3).

A more complete representation of the focal mechanism of an earthquake is given by the seismic moment (symmetric) tensor M_{ij} . For a pure double couple it can be defined, in the AR system, as a function of the outward normal and slip vectors of one of the nodal planes as

$$M_{ij}^{AR} = M_0 \begin{vmatrix} 2n_x d_x & n_x d_y + n_y d_x & n_x d_z + n_z d_x \\ n_y d_x + n_x d_y & 2n_y d_y & n_y d_z + n_z d_y \\ n_z d_x + n_x d_z & n_z d_y + n_y d_z & 2n_z d_z \end{vmatrix}. \tag{A.12}$$

In this case only four components are independent, while for a general composite mechanism the independent components of the moment tensor are 6.

Most of the CMT solutions available in the literature are given in the Harvard CMT coordinate system. The tensor can be expressed as a function of the six independent components reported on the CMT catalog ($M_{SS}, M_{EE}, M_{RR}, M_{SE}, M_{RS}, M_{RE}$) as

$$M_{ij}^{Harvard} = \begin{vmatrix} M_{SS} & M_{SE} & M_{RS} \\ M_{SE} & M_{EE} & M_{RE} \\ M_{RS} & M_{RE} & M_{RR} \end{vmatrix}. \tag{A.13}$$

As the direction of two coordinate axis (1 and 3) are reversed with respect to the AR System, the signs of the components 1–2 and 2–3 must be exchanged when passing from one to the other of the two systems

$$\begin{aligned} M_{12}^{AR} &= M_{21}^{AR} = -M_{12}^{Harvard} = -M_{21}^{Harvard}, \\ M_{23}^{AR} &= M_{32}^{AR} = -M_{23}^{Harvard} = -M_{32}^{Harvard}. \end{aligned} \tag{A.14}$$

The eigenvectors of the moment tensor corresponding to the most negative, most positive and intermediate eigenvalues coincide with the directions of the P -, T - and B -axis. Hence, these can be used to compute the nodal planes of the double couple best representing the mechanism. The latter however well represents the entire mechanism only when the most compressive and most tensional eigenvalues are close in modulus and the intermediate one is negligible with respect to them. Otherwise, the mechanism is complex and can be decomposed making some assumptions on the causative mechanics (see, Lay and Wallace, 1995; Julian et al., 1998, for a comprehensive discussion of different cases).

All decomposition methods require the removal of the isotropic tensor component. The result of this operation (preliminary done in most CMT catalogs) is the deviatoric moment tensor that in the major axis coordinate system is given by

$$\begin{vmatrix} \lambda'_1 & 0 & 0 \\ 0 & \lambda'_2 & 0 \\ 0 & 0 & \lambda'_3 \end{vmatrix} = \begin{vmatrix} \lambda_1 & 0 & 0 \\ 0 & \lambda_2 & 0 \\ 0 & 0 & \lambda_3 \end{vmatrix} - \begin{vmatrix} E & 0 & 0 \\ 0 & E & 0 \\ 0 & 0 & E \end{vmatrix}, \tag{A.15}$$

where $E = (\lambda_1 + \lambda_2 + \lambda_3)/3$. The most popular decomposition method subdivides the deviatoric moment tensor into the sum of two double couples. Assuming a decreasing ordering in modulus of deviatoric eigenvalues ($|\lambda'_1| > |\lambda'_2| > |\lambda'_3|$) we can write

$$\begin{vmatrix} \lambda'_1 & 0 & 0 \\ 0 & \lambda'_2 & 0 \\ 0 & 0 & \lambda'_3 \end{vmatrix} = \begin{vmatrix} M_0 & 0 & 0 \\ 0 & -M_0 & 0 \\ 0 & 0 & 0 \end{vmatrix} + \begin{vmatrix} 0 & 0 & 0 \\ 0 & M_1 & 0 \\ 0 & 0 & -M_1 \end{vmatrix}, \tag{A.16}$$

where $|M_0|$ and $|M_1|$ are the scalar seismic moment of major and minor double couples, respectively.

An alternative method, originally proposed by Knopoff and Randall (1970), decomposes the deviatoric moment tensor into the sum of a double couple and a CLVD with same P - and T -axis. Assuming again a decreasing ordering in modulus for the deviatoric moment tensor eigenvalues, this is given by

$$\begin{vmatrix} \lambda'_1 & 0 & 0 \\ 0 & \lambda'_2 & 0 \\ 0 & 0 & \lambda'_3 \end{vmatrix} = (1 - \eta) \begin{vmatrix} \lambda'_1 & 0 & 0 \\ 0 & -\lambda'_1 & 0 \\ 0 & 0 & 0 \end{vmatrix} + \eta \begin{vmatrix} \lambda'_1 & 0 & 0 \\ 0 & -\lambda'_1/2 & 0 \\ 0 & 0 & -\lambda'_1/2 \end{vmatrix}, \tag{A.17}$$

where $\eta = -2\lambda'_3/(\lambda'_1)$ is a measure of the size of the CLVD component with respect to the total deviatoric moment tensor. It may range from 0 for a pure double

couple to 1 for a pure CLVD. The scalar seismic moment of the double couple is given by $M_0 = (1 - \eta)|\lambda'_1| = |\lambda'_2 - \lambda'_3| = |\lambda'_1 - 2\lambda'_3|$.

A slightly different procedure is followed by the Harvard CMT and other routine catalogs. They compute the scalar moment M_{0b} of largest possible (best) double couple that has a CLVD remainder (Dziewonski et al., 1987) as the average of the two largest eigenvalues in modulus

$$M_{0b} = \frac{|\lambda'_1| + |\lambda'_2|}{2} = \frac{|\lambda'_1 - \lambda'_2|}{2}, \tag{A.18}$$

where the last passage is correct because the largest eigenvalue has opposed sign with respect to the other two due to the zero tensor trace and the assumed eigenvalues ordering. In this representation the isotropic moment tensor decomposes as

$$\begin{aligned} \begin{vmatrix} \lambda'_1 & 0 & 0 \\ 0 & \lambda'_2 & 0 \\ 0 & 0 & \lambda'_3 \end{vmatrix} &= \begin{vmatrix} (\lambda'_1 - \lambda'_2)/2 & 0 & 0 \\ 0 & (\lambda'_2 - \lambda'_1)/2 & 0 \\ 0 & 0 & 0 \end{vmatrix} \\ &+ \begin{vmatrix} -\lambda'_3/2 & 0 & 0 \\ 0 & -\lambda'_3/2 & 0 \\ 0 & 0 & \lambda'_3 \end{vmatrix}. \end{aligned} \tag{A.19}$$

The ratio between the sizes of CLVD remainder and total deviatoric moment tensor is now given by $\eta' = -\lambda'_3/(2\lambda'_1)$ that is exactly one-fourth of previous definition. Thus Eq. (A.19) can be written as

$$\begin{aligned} \begin{vmatrix} \lambda'_1 & 0 & 0 \\ 0 & \lambda'_2 & 0 \\ 0 & 0 & \lambda'_3 \end{vmatrix} &= (1 - \eta') \begin{vmatrix} \lambda'_1 & 0 & 0 \\ 0 & -\lambda'_1 & 0 \\ 0 & 0 & 0 \end{vmatrix} \\ &+ \eta' \begin{vmatrix} \lambda'_1 & 0 & 0 \\ 0 & \lambda'_1 & 0 \\ 0 & 0 & -2\lambda'_1 \end{vmatrix}. \end{aligned} \tag{A.20}$$

The lower limit of the ratio $\eta' = 0$ still corresponds to a pure double couple, while the upper one $\eta' = 0.25$ corresponds to a moment tensor apparently showing a pure CLVD mechanism. However, this decomposition scheme assumes that the double-couple component is dominating (75% of the size of total deviatoric moment tensor).

The latter scheme could be preferable if the CLVD remainder is the result of inversion errors whereas the previous one (Eq. (A.17)) could be more appropriate if the CLVD component has a physical origin.

References

Aki, K., Richards, P.G., 1980. *Quantitative Seismology*. W.H. Freeman and Company, San Francisco, 932pp.

Dziewonski, A.M., Chou, T.A., Woodhouse, J.H., 1981. Determination of earthquake source parameters from waveform data for studies of global and regional seismicity. *Journal of Geophysical Research* 86, 2825–2852.

Dziewonski, A.M., Ekström, G., Franzen, J.E., Woodhouse, J.H., 1987. Centroid-moment tensor solutions for January–March 1986. *Physics of the Earth and Planetary Interiors* 45, 1–10.

Julian, B.R., Miller, A.D., Foulger, G.R., 1998. Non-double-couple earthquakes 1. Theory. *Reviews of Geophysics* 36, 525–549.

Knopoff, L., Randall, M.J., 1970. The compensated linear vector dipole: a possible mechanism for deep earthquakes. *Journal of Geophysical Research* 75, 4957–4963.

Lay, T., Wallace, T.C., 1995. *Modern Global Seismology*. Academic Press, San Diego, 521pp.

Press, W.H., Flannery, B.P., Teukolsky, S.A., Vetterling, W.T., 1989. *Numerical Recipes. The Art of Scientific Computing (FORTRAN version)*. Cambridge University Press, Cambridge, 702pp.

Vannucci, G., Gasperini, P., 2003. A database of revised fault plane solutions for Italy and surrounding regions, *Computers & Geosciences*, this issue.